Multicomponent solute transport in soil lysimeters irrigated with waters of different quality

Maria C. Gonçalves,[1] Jirka Šimůnek,[2] Tiago B. Ramos,[1] José C. Martins,[1] Maria J. Neves,[1] and Fernando P. Pires[1]

Received 12 December 2005; revised 3 April 2006; accepted 21 April 2006; published 2 August 2006.

[1] A variety of analytical and numerical models have been developed during the past several decades to predict water and solute transfer processes between the soil surface and the groundwater table. While many models quantifying solute transport in soils usually consider only one solute and severely simplify various chemical interactions, others such as the geochemical module of HYDRUS-1D consider multiple solutes and their mutual interactions. In this study we use HYDRUS-1D to analyze water flow and solute transport in three soil lysimeters (1.2 m^2 × 1 m) irrigated during the summer months with waters of different quality that were used to evaluate salinization and alkalization hazards. The soil monoliths were constructed in a Eutric Fluvisol in Alentejo, Portugal. The electrical conductivity (EC) of irrigation water varied between 0.4 and 3.2 dS m^{-1}, and the sodium adsorption ratio (SAR) varied between 1 and 6 ($mmol_{(c)}$ $L^{-1})^{0.5}$, while maintaining a ratio of Ca:Mg equal to 1:2. The soil monoliths were subjected to regular rainfall and leaching during the rest of the year. Water contents and fluxes, concentrations of individual ions (Na^+, Ca^{2+}, and Mg^{2+}), electrical conductivity of the soil solution, SAR, and exchangeable sodium percentage (ESP) indices were monitored from May 2001 to September 2004 at four depths (10, 30, 50, and 70 cm) in all three soil monoliths. Irrigation water with EC up to 1.6 dS m^{-1} did not cause salinization or alkalization hazards. The rainfall water leached the salts accumulated during the irrigation period down to a depth of 100 cm. Rainfall, however, did not restore the salinity and sodicity of the soil to its original values below a depth of 60 cm for the lysimeter irrigated with water having an EC equal to 3.2 dS m^{-1}. HYDRUS-1D successfully described field measurements of the water content (R^2 = 0.60), overall salinity (R^2 = 0.65), and the concentration of individual soluble cations (R^2 ranged between 0.62 and 0.78) as well as the sodium adsorption ratio (R^2 = 0.87) and the exchangeable sodium percentage (R^2 = 0.76).

Citation: Gonçalves, M. C., J. Šimůnek, T. B. Ramos, J. C. Martins, M. J. Neves, and F. P. Pires (2006), Multicomponent solute transport in soil lysimeters irrigated with waters of different quality, *Water Resour. Res.*, *42*, W08401, doi:10.1029/2005WR004802.

1. Introduction

[2] Salinity is increasingly a concern in many irrigated areas of the Alentejo region of Southern Portugal where Mediterranean conditions prevail with high summer temperatures and scarce rainfall. Salinization (by irrigation water) is a process whereby soluble salts from the irrigation water accumulate in soil due to inadequate leaching, high water tables and/or high evaporation rates [*Keren*, 2000]. The water quality in several reservoirs of the region at present time varies between about 0.4 (Campilhas, Alto Sado, Odivelas) and 1.6 dS m^{-1} (Roxo), although higher values (to about 2.6 dS m^{-1}) have been frequently observed in Roxo over the years. Many irrigated areas in the region will be integrated in the near future within the Alqueva project, such that additional 110,000 ha of agricultural land will be irrigated from a newly constructed dam on the Guadiana river. This river is one of the largest in the southern Iberian Peninsula, with flow rates that exhibit large seasonal and interannual fluctuations. Large changes in river water quality are due to changes in the flow rate, the local climate with frequent dry years, the existence of 300,000 ha of irrigated fields in Spain's upstream catchment area, and the existence of several urban agglomerations. As water is being used and reused, risks of soil salinization for irrigated soils undoubtedly will worsen. A sound irrigation policy must be established to mitigate these risks. Such policy must be based on a quantitative understanding of the subsurface movement of water and dissolved chemicals. Modeling of subsurface water flow and the transport of major soluble ions in and below the root zone is essential for predicting groundwater quality, implementing better irrigation and fertilization practices, and quantifying salinization and alkalization hazards.

[1] Department of Soil Science, Estação Agronómica Nacional, Oeiras, Portugal.
[2] Department of Environmental Sciences, University of California, Riverside, California, USA.

0043-1397/06/2005WR004802$09.00

Table 1. Chemical Species Included in the Major Ion Module of HYDRUS-1D

	Number of Species	Ions
Aqueous components	6	Ca^{2+}, Mg^{2+}, Na^{+}, K^{+}, SO_4^{2-}, Cl^{-}
Complexed species	10	$CaCO_3^{\circ}$, $CaHCO_3^{+}$, $CaSO_4^{\circ}$, $MgCO_3^{\circ}$, $MgHCO_3^{+}$, $MgSO_4^{\circ}$, $NaCO_3^{-}$, $NaHCO_3^{\circ}$, $NaSO_4^{-}$, KSO_4^{-}
Precipitated species	6	$CaCO_3$, $CaSO_4 \cdot 2H_2O$, $MgCO_3 \cdot 3H_2O$, $Mg_5(CO_3)_4(OH)_2 \cdot 4H_2O$, $Mg_2Si_3O_{7.5}(OH) \cdot 3H_2O$, $CaMg(CO_3)_2$
Sorbed (exchangeable) species	4	Ca, Mg, Na, K
CO_2-H_2O species	7	P_{CO2}, H_2CO_3*, CO_3^{2-}, HCO_3^{-}, H^{+}, OH^{-}, H_2O

[3] The past several decades have seen considerable progress in quantifying water flow and solute transport processes in the unsaturated zone [*van Genuchten and Šimůnek*, 2004]. A large number of analytical and numerical models are now available to predict flow and transport processes between the soil surface and the groundwater table. These models are typically based on the numerical solutions of the Richards equation for variably saturated flow, and analytical or numerical solutions of the Fickian-based convection-dispersion equation for solute transport. Deterministic solutions of these classical equations likely will remain important tools for predicting water and solute movement in the vadose zone, and for analyzing specific laboratory or field experiments involving unsaturated water flow and solute transport. Models of this type are also helpful tools for extrapolating information from a limited number of field experiments to different soil types, crop and climatic conditions, as well as to different tillage and water management schemes. Unfortunately, evaluation of these models under field conditions is still very limited, in large part because of their need for a variety of input data, including soil hydraulic properties, solute transport parameters, parameters characterizing the partitioning between the solid phase and the soil solution, and meteorological and crop related information.

[4] While many models have been developed over the years, most consider the transport of only one solute and severely simplify various chemical interactions [*Šimůnek and Valocchi*, 2002]. The relatively complex processes of adsorption and cation exchange are often accounted for by means of empirical linear or nonlinear adsorption isotherms. Other processes such as precipitation/dissolution and biodegradation are frequently simulated by invoking simplified first- or zero-order rate equations. During the last two decades several models have been developed that can consider multiple solutes and their various interactions, such as precipitation/dissolution and competition for sorption sites. *Šimůnek and Valocchi* [2002] divided these multicomponent solute transport models into two large groups: general models and models with specific chemistry. Models with generalized chemistry provide users considerable freedom in terms of designing their particular chemical system, and thus permit a relatively broad range of applications. On the other hand, models with specific chemistry are much more restrictive in terms of the prescribed (and often simplified) chemical system, and thus are generally constrained to very specific applications. However, they are often much easier to use and computationally much more efficient than general models.

[5] Models simulating the transport of major ions are typical examples of models with specified chemistry. For example, *Robbins et al.* [1980a, 1980b] developed chemical precipitation-dissolution and cation exchange subroutines using equilibrium chemistry and coupled them with a one-dimensional unsaturated water flow model. Their model was tested against experimental data from a lysimeter study. *Dudley et al.* [1981] further evaluated this same model for field conditions under cropped and uncropped conditions. They obtained adequate predictions of total salinity but not of individual ion concentrations. The salinity model of *Robbins et al.* [1980a] was later used also by *Russo* [1986] to theoretically investigate the leaching of a gypsiferous-sodic soil using different water qualities. Robbins' equilibrium chemistry model additionally formed a basis for the LEACHM numerical code of *Wagenet and Hutson* [1987].

[6] *Šimůnek et al.* [1996] and *Šimůnek and Suarez* [1994] later coupled a major ion chemistry module (Table 1 lists considered species) with one- and two-dimensional variably saturated water flow models, respectively, while also considering solute transport, carbon dioxide transport, and heat flow. The resulting UNSATCHEM models considered the effects of CO_2 producing microbiological activity and CO_2 transport in the soil on geochemical transport. Contrary to models based on the geochemical module of *Robbins et al.* [1980a], the UNSATCHEM models can consider kinetic chemical reactions (precipitation/dissolution of calcite and dissolution of dolomite). They can also be used to evaluate chemical reactions for solutions having very high ionic strengths since they evaluate activity coefficients either using an extended version of the Debye-Hückel equation [*Truesdell and Jones*, 1974] for dilute to moderately saline solutions, or by means of the Pitzer expressions [*Pitzer*, 1979]. The major ion chemistry and carbon dioxide modules of UNSATCHEM were recently incorporated in the HYDRUS-1D software package [*Šimůnek et al.*, 2005]. This model thus represents a relatively powerful tool for evaluating major ion chemistry in the subsurface, for assessing the effects of irrigation water quality on groundwater recharge, and for quantitative predictions of the amount of water and amendment required in order to reclaim sodic and saline soils to desired levels of salinity and ESP (exchangeable sodium percentage) [*Šimůnek and Suarez*, 1997; *Šimůnek and Valocchi*, 2002]. While the water flow and solute transport components of HYDRUS-1D have been used widely in both research and management, application of the major ion chemistry module has been much more limited. A majority of applications dealt

Table 2. Ionic Composition of Irrigation Waters Applied to the Soil Monoliths and Their Classification According to U.S. Salinity Laboratory[a]

Monolith	EC, dS m^{-1}	SAR, $(mmol_{(c)}\ L^{-1})^{0.5}$	Ca^{2+}, $mmol_{(c)}\ L^{-1}$	Mg^{2+}, $mmol_{(c)}\ L^{-1}$	Na^{+}, $mmol_{(c)}\ L^{-1}$	Cl^{-}, $mmol_{(c)}\ L^{-1}$	USSL Classification[b]
Waters I							
A	0.3	1.0	1.00	1.00	1.00	3.00	C2-S1
B	0.8	3.0	1.28	2.56	4.16	8.00	C3-S1
C	1.6	6.0	1.93	3.86	10.21	16.00	C3-S2
Waters II							
A′	0.8	1.5	1.85	3.65	2.50	8.00	C3-S1
B′	1.6	3.0	3.16	6.32	6.52	16.00	C3-S1
C′	3.2	6.0	5.10	10.20	16.70	32.00	C4-S2

[a] *Richards* [1954].
[b] C2, medium-salinity water (EC 0.25–0.75 dS m^{-1}); C3, high-salinity water (EC 0.75–2.25 dS m^{-1}); C4, very high salinity water (EC >2.25 dS m^{-1}); S1, low-sodium water [SAR 0–10 $(mmol_{(c)}\ L^{-1})^{0.5}$]; S2, medium-sodium water [SAR 10–18 $(mmol_{(c)}\ L^{-1})^{0.5}$].

mainly with hypothetical examples [e.g., *Šimůnek and Suarez*, 1994, 1997] because of a lack of appropriate experimental data.

[7] The objective of this study was to carry out field experiments to quantify salinization and alkalization risks of a medium-textured Eutric Fluvisol, irrigated with waters of different qualities, in Alvalade-Sado (Alentejo) region of Portugal. We also evaluated the effectiveness of the HYDRUS-1D software package [*Šimůnek et al.*, 2005] to predict water contents and fluxes, concentrations of individual ions, the overall salinity given by the electrical conductivity (EC), as well as SAR (sodium adsorption ratio) and ESP (exchangeable sodium percentage) under field conditions.

2. Materials and Methods

2.1. Field Experimental Conditions

[8] Salinization and alkalization processes were studied on soils irrigated with three waters of different quality in Alvalade do Sado, Alentejo, Portugal. Three soil monoliths (1.2 m^2 × 1.0 m deep) were for this purpose constructed in a Eutric Fluvisol [*Food and Agricultural Organization*, 1998]. The monoliths were laterally isolated with plastic to prevent lateral water and solute fluxes and subjected to atmospheric conditions at the top and free drainage conditions at the bottom. The soil monoliths were covered by annual spontaneous vegetation (gramineous plants, leguminosae and compositae). TDR probes using waveguides from the Trase System (Soil Moisture Equipment Corp., Goleta, CA) and ceramic cups were installed in each soil monolith in two replicates at depths of 10, 30, 50 and 70 cm.

[9] The monoliths were manually irrigated from 2001 to 2004 during the normal irrigation period between May and September. Application amounts were 10 mm each, for a total of 500 mm per year. The monoliths were exposed to natural atmospheric conditions (rainfall and evapotranspiration) during the rest of the year. Because of variable Mediterranean conditions, large annual differences existed in the cumulative rainfall between September and May, which corresponds with the soil's main leaching cycle. Rainfall totals in this time period ranged from 445 mm in 2001–2002, 587 mm in 2002–2003, to 481 mm in 2003–2004. In order to easily collect soil solution samples, the soil water content was kept between 25 and 35% (pressure heads of −500 and −40 cm, respectively) during the irrigation period. This water content interval corresponds approximately with the soil field capacity. Irrigation water compositions, named A, B, and C according to the monolith to which they were applied, are described in Table 2. Waters that were used in the first 2 years (waters I: B and C) were obtained by adding increasing concentrations of NaCl, $CaCl_2$ and $MgCl_2$ to water A available in the region, using a ratio of 1:2 for Ca:Mg. The electrical conductivity (EC) of the three waters was increased in 2003 and 2004, while maintaining the same balance between the cations (waters II: A′, B′, and *C*′).

[10] Soil solutions were collected from ceramic cups, while soil water contents were monitored using TDRs at four depths twice a week during the irrigation periods and once a week during the remaining months. At the beginning of the experiment, at the end of each irrigation period, and after the following winters, soil samples were collected at 5 depths (0–20, 20–40, 40–60, 60–80, and 80–100 cm) to measure the exchangeable cations, and the cation exchange capacity (CEC).

2.2. Input Data

2.2.1. Evapotranspiration

[11] The experimental field was located 10 m from a meteorological station. Collected meteorological data were used to determine the potential evapotranspiration rate (ET_0) using the Penman-Monteith method [*Allen et al.*, 1998]. A crop coefficient (K_c), which accounts for both crop transpiration and soil evaporation, was used to calculate crop evapotranspiration. The crop evapotranspiration rate (ET_c), being the product of ET_0 and K_c, was calculated using K_c values for pasture (0.4 for early growth stages, 0.85 for periods without irrigation [*Allen et al.*, 1998] and 1.0 when irrigated, since during each irrigation period the soil water content was kept at the field capacity). The leaf area index (LAI) (a mean value of 3.5 $m^2\ m^{-2}$) and a corresponding soil cover factor (SCF) were used to account for different stages of the soil cover and to divide the ET_c daily values into crop transpiration (T) and soil evaporation (E) rates.

2.2.2. Root Distribution

[12] Evaporation and plant transpiration exert a major influence on water and solute distributions in near-surface environments. These processes concentrate salts by decreasing the amount of water in the soil, which, when combined

Table 3. van Genuchten–Mualem Parameters for the Soil Hydraulic Functions[a]

	Depth, cm		
	0–48	48–85	85–170
θ_r, cm^3 cm^{-3}	0.050	0.108	0.000
θ_s, cm^3 cm^{-3}	0.427	0.428	0.373
α, cm^{-1}	0.029	0.108	0.040
N	1.21	1.16	1.15
ℓ	−4.39	−5.91	−6.91
K_s, cm d^{-1}	18.2	99.3	21.4
R^2	0.995	0.994	0.998

[a]R^2 is the regression coefficient between measured and fitted soil hydraulic property data.

with irrigation in arid regions, can lead to highly saline conditions. For this reason it is important to consider the root distribution in the soil profile. Roots of the existing vegetation in the top of the soil monolith were not very deep, except for a few plants. On the basis of field observations that showed a relatively uniform rooting depth of 30 cm, with only a small fraction of roots extending below this depth, we assumed that 80% of all roots were distributed in the first 30 cm of the soil profile and that the remaining 20% extended to a depth of 70 cm.

2.2.3. Soil Hydraulic Properties

[13] Disturbed and undisturbed samples (100, 200, and 4700 cm^3) were collected at the beginning of the experiment from different soil layers to measure the unsaturated soil hydraulic properties (i.e., the soil water retention and hydraulic conductivity functions). The soil water retention curve was determined using suction tables with sand or kaolin for suctions below 500 cm and a pressure plate apparatus for suctions above 1000 cm. The hydraulic conductivity curve was obtained by combining measurements on the 4700 and 200 cm^3 samples. A constant head method was used to measure the saturated hydraulic conductivity. The crust method [*Bouma et al.*, 1983] was used to measure the unsaturated hydraulic conductivity on larger samples, while the hot air method [*Arya et al.*, 1975] was used at greater suctions to measure unsaturated hydraulic conductivities on 200 cm^3 samples. The soil hydraulic functions were described using the van Genuchten-Mualem equations [*van Genuchten*, 1980], with their parameters optimized using the RETC code [*van Genuchten et al.*, 1991]. Table 3 lists the van Genuchten-Mualem parameters that describe the soil hydraulic functions for the analyzed soils. The saturated hydraulic conductivities in Table 3 were assumed to represent optimum hydraulic conditions; they were reduced during the calculations using the reduction functions of *McNeal* [1968] to account for the adverse effects of the solution composition.

2.2.4. Solute Transport Parameters

[14] The solute transport parameters (dispersivities) were obtained from solute displacement experiments carried out on undisturbed 9040 cm^3 cylindrical samples with a cross-sectional area of 452 cm^2. A 0.05 M KCl pulse was applied during steady state saturated flow. The sampling and preparation of the soil columns were carried out as described by *Mallants et al.* [1994]. All experimental procedures are explained by *Gonçalves et al.* [2001]. The chloride breakthrough curves were expressed using the dimensionless concentration as a function of the number of pore volumes leached through the soil column. Dispersivity values (Table 4) were obtained with the nonlinear parameter estimation code CXTFIT 2.1 of *Toride et al.* [1995] by fitting analytical solutions of the CDE to observed breakthrough data.

2.2.5. Physical and Chemical Analysis

[15] The particle size distribution was obtained using the pipette method for particles with diameters less than 20 μm (clay and silt fractions) and by sieving for particles between 200 and 2000 μm (coarse sand) and between 20 and 200 μm (fine sand). The dry bulk density (ρ_b) was obtained by drying volumetric soil samples at 105°C. Concentrations of soluble cations Na^+, Ca^{2+}, and Mg^{2+} in the soil solutions collected with the ceramic cups and from saturation extracts were measured using atomic absorption spectrophotometry. The electrical conductivity and Cl^- concentrations were determined potentiometrically. Exchangeable cations and cation exchange capacity (CEC) were determined with a modified Melich method [*Melich*, 1948] using a solution of $BaCl_2$+triethanolamine at pH 8.1. The pH was measured on a suspension of soil and distilled water (1:2.5 w/v soil/solution) using a potentiometric method [*Van Lierop*, 1990]. Gapon selectivity coefficients [*White and Zelazny*, 1986] describing the partitioning between the solid phase and the solution were calculated from the initial soil conditions. Table 4 presents the main physical and chemical characteristics of the soil.

3. Data Analyses

[16] The experimental data were analyzed using version 3.0 of the HYDRUS-1D software package [*Šimůnek et al.*,

Table 4. Physical and Chemical Soil Characteristics (Initial Conditions)[a]

	Depth, (c)		
	0–48	48–85	85–170
Coarse sand, g kg^{-1}	62	51	61
Fine sand, g kg^{-1}	532	468	428
Silt, g kg^{-1}	296	292	282
Clay, g kg^{-1}	110	189	229
Texture	Silty-loam	Silty-loam	Loam
Bulk density, g cm^{-3}	1.49	1.51	1.61
EC, dS m^{-1}	0.20	0.23	0.23
pH (H_2O)	5.94	6.58	6.74
Soluble cations, mmol$_{(c)}$ L^{-1}			
Ca^{2+}	0.753	0.673	0.670
Mg^{2+}	0.613	0.560	0.520
Na^+	0.625	0.990	1.000
Cl^-,[b] mmol$_{(c)}$ L^{-1}	1.991	2.223	2.190
Exchangeable cations, mmol$_{(c)}$ kg^{-1}			
Ca^{2+}	46.63	58.50	62.00
Mg^{2+}	21.88	27.00	28.13
Na^+	1.45	2.16	2.17
CEC, mmol$_{(c)}$ kg^{-1}	69.96	87.66	92.30
SAR, (mmol$_{(c)}$ L^{-1})$^{0.5}$	0.756	1.260	1.296
ESP, %	2.00	2.46	2.35
K (Na/Ca), (mol L^{-1})$^{-1/2}$	1.93	1.37	1.28
K, Mg/Ca	0.52	0.50	0.51
Dispersivity, cm	5.36	0.68	12.18

[a]EC, electrical conductivity; CEC, cation exchange capacity; SAR, sodium adsorption ratio; ESP, exchangeable sodium percentage; K, Gapon selectivity coefficient.

[b]Calculated to maintain the charge balance.

2005]. In addition to one-dimensional variably saturated water flow, and solute and heat transport, this program also numerically simulates the transport of carbon dioxide and major ions, and their mutual interactions. The program numerically solves the Richards equation describing variably saturated water flow and various forms of the convection-dispersion equation describing the transport of heat, solutes, and carbon dioxide. The flow equation incorporates a sink term to account for water uptake by plant roots. Water and salinity stress response functions that reduce the potential root water uptake can be defined according to functions proposed by *Feddes et al.* [1978] or *van Genuchten* [1987]. Although the program considers multiple analytical models to represent the soil hydraulic properties, in this study we used only *van Genuchten*'s [1980] analytical model. This model requires six parameters, i.e., the residual, θ_r, and saturated, θ_s, water contents, the saturated hydraulic conductivity K_s, the tortuosity factor l, and two shape parameters α and n. Atmospheric and free drainage boundary conditions were used at the surface and bottom of the soil profile, respectively. Atmospheric boundary conditions require specification of daily values of precipitation, irrigation, evaporation, and transpiration. The governing equations for all simulated processes, possible initial and boundary conditions, and other details can be obtained from *Šimůnek et al.* [2005].

[17] HYDRUS-1D was recently updated with a major ion chemistry module extracted from the UNSATCHEM model [*Šimůnek and Suarez*, 1994; *Šimůnek et al.*, 1996]. The geochemical module considers the transport of seven major ions (six aqueous components in Table 1, and alkalinity) and various temperature-dependent equilibrium chemical reactions between these ions, such as aqueous complexation, precipitation and dissolution of several solid phases, and cation exchange. Although the geochemical module has been extended to other species (e.g., boron and silica species by *Suarez and Šimůnek* [1997] or Fe and As by *Decker et al.* [2006]), in this study we will consider only major ions. The aqueous complexes and mineral species included in the geochemical module of HYDRUS-1D are compiled in Table 1, while thermodynamic coefficients, kinetic reaction constants, and other details are provided in *Šimůnek et al.* [1996, 2005].

[18] Since during our experiment and modeling analyses we did not observe any precipitation or dissolution of mineral phases, we will not discuss these further. The two most important chemical reactions in our application were aqueous complexation and cation exchange. Equations for the aqueous complexation reactions can be obtained using the law of mass action. Partitioning between the solid exchange phase and the solution phase (cation exchange reaction) is described in HYDRUS by the Gapon exchange equation [*White and Zelazny*, 1986]. As an example, for the case of exchange of the cations Ca^{2+} and Na^{+}, i.e.,

$$2\,\overline{c_{\mathrm{Na}}^{+}} + c_{\mathrm{Ca}}^{2+} \Leftrightarrow \overline{c_{\mathrm{Ca}}^{2+}} + 2\,c_{\mathrm{Na}}^{+} \tag{1}$$

we used the following Gapon equation

$$K_{\mathrm{Ca/Na}} = \frac{\overline{c_{\mathrm{Ca}}^{2+}}}{\overline{c_{\mathrm{Na}}^{+}}} \frac{\gamma_{\mathrm{Na}} c_{\mathrm{Na}}^{+}}{\left(\gamma_{\mathrm{Ca}} c_{\mathrm{Ca}}^{2+}\right)^{1/2}} \tag{2}$$

It is further assumed that the cation exchange capacity $\overline{c}_T$ (or CEC) was constant and independent of pH. When exchanger phase concentrations are expressed in equivalents per mass of solid, then

$$\overline{c}_T = \sum_{i=1}^{M_z} \overline{c}_i \tag{3}$$

where M_z is the number of ion exchange species.

[19] The sodium adsorption ratio (SAR) was calculated as follows:

$$SAR = \frac{(Na^{+})}{\sqrt{\frac{(Ca^{2+} + Mg^{2+})}{2}}} \tag{4}$$

where Na^{+}, Ca^{2+}, and Mg^{2+} are the cation concentrations in $\mathrm{mmol_{(c)}\ L^{-1}}$ (millimol of charge per liter is an SI unit corresponding to milliequivalent per liter). We further used the exchangeable sodium percentage (*ESP*), which is defined as the ratio of exchangeable Na to the sum of exchangeable cations, expressed in equivalents per mass of solid:

$$\mathrm{ESP} = \frac{\overline{\mathrm{Na}}^{+}}{(\mathrm{CEC})} 100 \tag{5}$$

The electrical conductivity in HYDRUS was determined from individual anions and cations following the method of *McNeal et al.* [1970], while the osmotic coefficient ϕ was calculated using the semiempirical equation of *Pitzer* [1973].

[20] The accumulation of monovalent cations, such as sodium and potassium, or the use of high-quality water, often leads to clay dispersion or swelling. These processes can have an adverse effect on the soil hydraulic properties including hydraulic conductivity, infiltration rates and soil water retention as a result of swelling and clay dispersion. These negative effects are usually explained based on the diffuse double layer theory [*Russo and Bresler*, 1977; *Russo*, 1988]. They become more pronounced with decreasing salt concentration and the valence of the adsorbed ions [*Shainberg and Levy*, 1992]. HYDRUS accounts for these adverse effects on the hydraulic conductivity by using reduction functions developed by *McNeal* [1968] (see description by *Šimůnek et al.* [1996, 2005]):

$$K(h, \mathrm{SAR}, C_0) = r(\mathrm{SAR}, C_0) K(h) \tag{6}$$

where $K(h)$ is the hydraulic conductivity function, C_0 is the total salt concentration of the ambient solution in $\mathrm{mmol_c L^{-1}}$, and r is a scaling factor which represents the effect of the solution composition (SAR and dilution) on the final hydraulic conductivity (dimensionless), and which is related to SAR and salinity. The hydraulic conductivity without the scaling factor r can be assumed to be the optimal value under favorable chemical conditions in terms of optimal SAR and salinity.

[21] In addition to a visual check, field-measured values were compared with results of the HYDRUS-1D predictions using simple regression analysis (R^2). Regression analyses between measured and simulated data were carried out for

water contents, electrical conductivities of the soil solution (representing the overall salinity), for the individual ion concentrations (Na^+, Ca^{2+}, Mg^{2+}), and for the SAR and ESP relationships. The analyses were carried out for a particular variable within the overall data set (all depths combined), as well as using data of the individual depths.

4. Results and Discussion

4.1. Volumetric Water Contents

[22] The experiments started on 23 May 2001 (day 1). As initial conditions for the HYDRUS-1D simulations we used TDR water content readings of 0.1775, 0.2140, 0.2605, 0.2828 cm^3 cm^{-3} at 10, 30, 50, and 70 cm depths, respectively, immediately before the start of the irrigation period. Other input for HYDRUS-1D consisted of the soil hydraulic parameters for the three soil horizons, water applied to the top of three monoliths either from irrigation or rainfall, and daily ET_c values divided into separate evaporation (E) and transpiration (T) components. Simulations were carried for a time period of four years. Although the initial water contents varied slightly between the three monoliths, all other parameters and properties were very much the same, which allowed us to assume in our initial calculations that one single HYDRUS-1D simulation could well characterize all three monoliths. We thus neglected any possible effects of different irrigation waters on root water uptake and plant growth. Figure 1 shows for the three monoliths the mean values and standard deviations of the water contents measured with TDRs at depths of 10, 30, 50, and 70 cm, and compares these values with results of the HYDRUS-1D simulation between 23 May 2001 and 30 September 2004 (i.e., 1227 days).

[23] During the four irrigation periods (i.e., from day 1 to 76; 388 to 479; 737 to 820; and 1128 to 1186), TDR measurements showed water content values near the field capacity (0.25 to 0.35 cm^3 cm^{-3}) and then gradually decreasing values until the beginning of the rainy seasons (days 134–323, 480–713, and 861–1084) when they started to increase again. Overall, simulated water contents closely mirrored measured values at all four depths (Figure 1). When comparing measured and simulated values, one must realize that water contents were measured only sporadically and never during or immediately after rainfall events, thus avoiding the highest water content values. On the other hand, HYDRUS-1D calculates the entire process and predicts continuous water contents during all events, including possible extremes.

[24] The relationship between measured and simulated water contents at four depths in all three monoliths was analyzed by fitting a linear model to the data. Regression coefficients were calculated for each layer and for all layers combined. An overall regression coefficient (R^2) of 0.60 was obtained for all n = 1180 observations combined, while values for the individual layers decreased with depth from 0.66 to 0.42 (Table 5). Better correspondence between measured and simulated values probably could have been obtained using the inverse (parameter estimation) option of HYDRUS-1D [*Šimůnek et al.*, 2005]. However, since our goal was to use as much as possible independently measured parameters, the parameter estimation option of HYDRUS-1D was not used for our water flow simulations.

[25] In subsequent simulations involving the transport of major ions, we considered the possible effects of different irrigation waters (and soil solution compositions) on hydraulic conductivities and root water uptake.

4.2. Overall Salinity

[26] Since the soil used in our experiments (a medium textured Fluvisol) had favorable hydraulic characteristics (saturated hydraulic conductivities of about 18, 100, and 22 cm d^{-1} in the 0–48, 48–75, and 75–120 cm depths, respectively; see Table 3) and because of leaching during the winter rain seasons, the use of irrigation waters up to 1.6 dS m^{-1} (monoliths A and B) did not lead to soil salinization (Figure 2). Only at the end of each irrigation cycle did the soil salinity increase to 5–6 dS m^{-1} in the upper soil layers (0–40/50 cm). The salinity of the deeper horizons increased during and after the rainfall periods, often reaching 3 dS m^{-1}, due to leaching of salts from the upper layers.

[27] The application of irrigation water C′ (EC = 3.2 dS m^{-1}) during the last two irrigation periods had the biggest effect on the soil solution salinity, leading to a value of about 12 dS m^{-1} in the 0–20 cm layer. During the subsequent rainfall period (between 864 to 1084 days), salinity values increased to about 10 dS m^{-1} in layers below the 50-cm depth due to leaching of salts from upper layers. Such EC values can lead to significant yield reductions for a large number of crops, especially vegetables [e.g., *Ayers and Westcot*, 1985; *Mass*, 1990; *Steppuhn et al.*, 2005].

[28] HYDRUS-1D simulations of the total soil salinity resulted in a generally good agreement with the observed patterns in all three soil monoliths. Figure 2 shows observed and simulated total soil salinities for four layers of monoliths A, B and C. We often lacked measured data between the end of the irrigation period and the beginning of the rainfall period. During this time period, which lasted about 2 months, soil water contents decreased significantly below field capacity due to relatively high air temperatures and soil evaporation rates, which prevented us from extracting soil solution samples with ceramic cups. Although the measured data hence could not validate the simulated EC peaks, the calculated values are reasonable and to be expected during periods of decreasing or low water contents caused by evapotranspiration. A value of 0.65 for R^2 (for n = 1039 observations) was obtained for the relation between measured and simulated EC values (Table 5). Table 5 also provides regression coefficients calculated for each depth from the observed and simulated data.

4.3. Individual Cations

[29] Measured and simulated concentrations of soluble Na^+, Ca^{2+} and Mg^{2+} for the three monoliths at four depths (10, 30, 50, and 70 cm) are presented in Figures 3, 4, and 5, respectively. The general behavior of sodium is the same as that of the electrical conductivity in Figure 2. Na^+ concentrations increased gradually at all depths during the irrigation cycles, and peaked during the following dry periods before the winter rainfalls. The highest concentrations were reached in monolith C with the application of the lowest-quality water (C′). The peak Na^+ concentration was about 40 $mmol_{(c)}$ L^{-1}, which is more than double the concentration of the irrigation water. Sodium concentrations subsequently decreased during the rainfall periods in the two

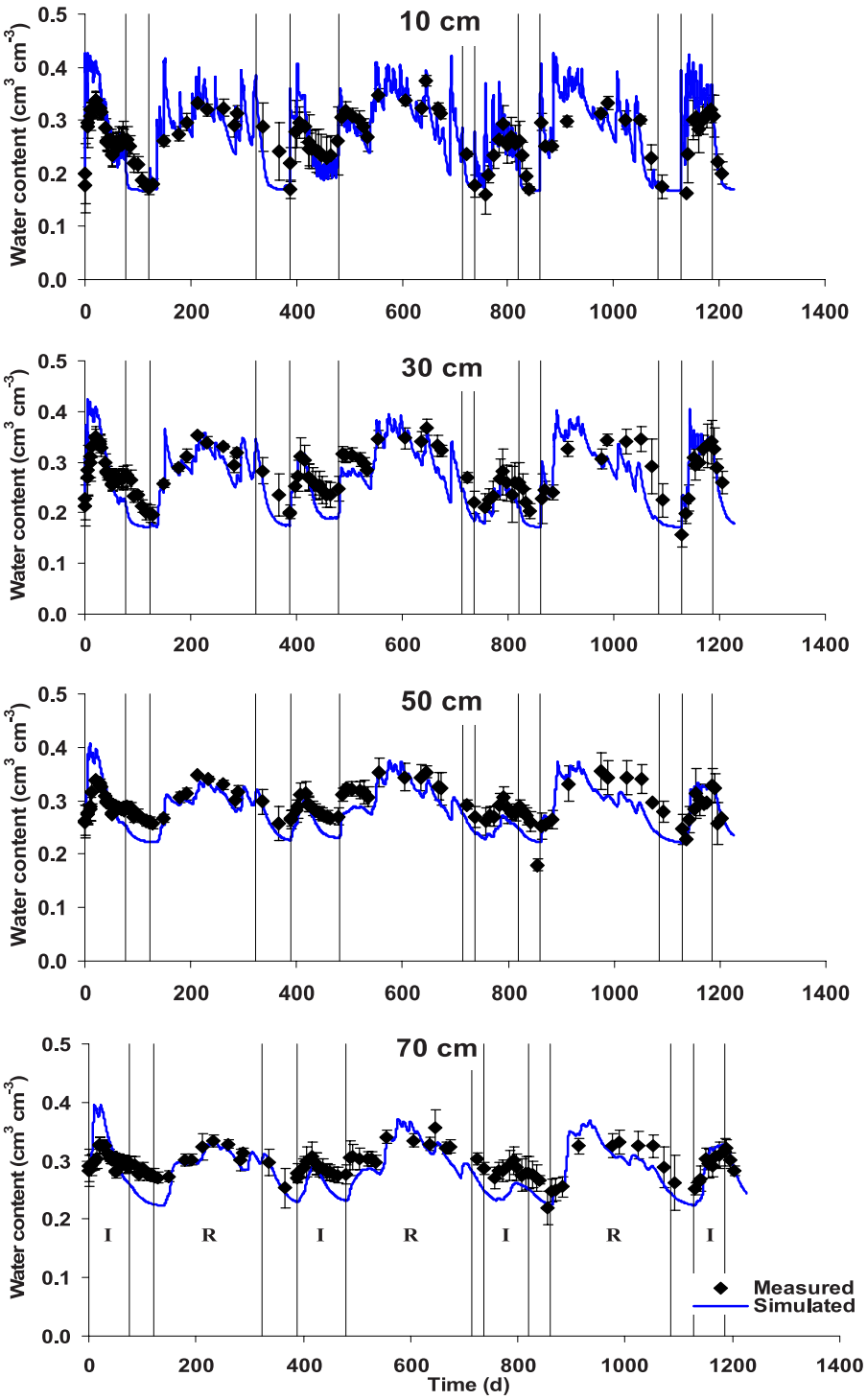

Figure 1. Measured (TDR) and simulated (Hydrus) volumetric water contents at 10, 30, 50, and 70 cm depths. I and R denote the irrigation and rainfall periods, respectively.

surface layers (10 and 30 cm), reaching values similar to the initial conditions. The deeper depths (50 and 70 cm) showed an increase in sodium content due to the leaching from the upper layers. In addition to the sudden increases in Na^+ concentrations during the winter periods, a gradual increase in Na occurred in deeper layers during the entire experiment.

[30] HYDRUS-1D simulations of the sodium concentrations resulted in a generally very good agreement with measured values in all three monoliths. A value of 0.78 for R^2 was obtained between measured and simulated sodium concentrations for the 1080 observation data points (Table 5).

[31] Figures 4 and 5 present results for calcium and magnesium concentrations, respectively. Once again, the general dynamics of the Ca and Mg concentrations during the experiments was similar to those for sodium and EC.

Table 5. Results of Regression Analyses Between Measured and Simulated Soil Water Contents, Soluble Na^+, Mg^{2+}, and Ca^{2+} Concentrations, Electrical Conductivities of the Soil Solution, Sodium Adsorption Ratios, and Exchangeable Sodium Percentages[a]

	Lysimeter Layers											
	10		30		50		70		90		Overall	
Parameters	R^2	n	R^2	n	R^2	n	R^2	n	R^2	n	R^2	n
Water content	0.66	259	0.69	310	0.53	286	0.42	325	-	-	0.60	1180
Na^+	0.84	277	0.71	269	0.82	272	0.78	262	-	-	0.78	1080
Ca^{2+}	0.73	271	0.51	249	0.54	255	0.76	240	-	-	0.63	1015
Mg^{2+}	0.79	293	0.53	256	0.46	256	0.68	250	-	-	0.62	1055
EC	0.87	274	0.53	261	0.60	254	0.70	250	-	-	0.65	1039
SAR	0.88	264	0.84	292	0.87	312	0.74	311	-	-	0.87	1180
ESP	0.81	24	0.84	24	0.77	24	0.87	24	0.49	24	0.76	120

[a]Regression coefficients R^2 were calculated both for the different layers and for all layers combined; n is the number of data points used in the regression analyses.

However, the correspondence between measured and simulated values for these two cations was somewhat less than for sodium. The calculated R^2 value was equal to 0.63 for calcium (n = 1015) and 0.62 for magnesium (n = 1055) (Table 5). The largest differences were found at a depth of 70 cm between days 952 and 1073 for both calcium and magnesium in all three monoliths. Smaller but noticeable differences were also observed for sodium at the same times and depth. This disagreement could be caused by experimental errors in the soil solution extraction process. However, a more likely explanation is that roots during this time interval reached this deeper soil horizon and extracted here more water than was considered by the model. Notice that the calculated water contents were overpredicted during this time period at this depth, resulting in underpredictions of the cation concentrations. Nevertheless, visual inspection and the obtained R^2 values suggest relatively good overall correspondence between measured and simulated data.

4.4. Sodium Adsorption Ratio

[32] Figure 6 presents results for the measured and simulated SAR values. For this variable we obtained the largest regression coefficient (R^2 = 0.87 for n = 1180) between measured and simulated values (Table 5). Relatively large SAR values were observed during time periods when lysimeters were irrigated with C and C′ waters at depths of 10 and 30 cm. The maximum SAR value, about 9 $(mmol_{(c)}\ L^{-1})^{0.5}$, was obtained for the first layer of monolith C when irrigated with water C'. During the following winter season, the SAR of this first layer decreased to about 5 $(mmol_{(c)}\ L^{-1})^{0.5}$ due to the leaching by rainwater. The value of 5 $(mmol_{(c)}\ L^{-1})^{0.5}$ is about 6 times larger than the initial SAR values in the soil profile (i.e., 0.8 $(mmol_{(c)}\ L^{-1})^{0.5}$). Winter leaching, however, led to an increase in SAR in the deeper horizons. SAR gradually increased with time at depths of 50 and 70 cm of monolith C without any visible fluctuations.

[33] Similar trends were observed for the other two monoliths (A and B), although the SAR values were mostly much lower. A gradual increase in SAR with time at the 30, 50 and 70 cm depths was observed in monolith B, especially after day 800 when the quality of the irrigation water decreased. SAR fluctuations at 10 cm depth were similar as in the monolith C, exhibiting larger values during the irrigation periods and lower values during the winter rainfall seasons.

[34] SAR is an integral variable that characterizes salt-affected soils and provides information on the comparative concentrations of Na^+, Ca^{2+}, and Mg^{2+} in soil solutions. This variable takes into consideration that the adverse effects of sodium are moderated by the presence of calcium and magnesium ions. SAR reflects relatively complex processes in the soil profile that, at least in our study, were dominated by cation exchange. SAR gradually increased with time at different depths after 800 days when the quality of the irrigation water changed. However, the increase was delayed since the SAR front moves slower than the concentration fronts of nonreactive solutes, such as Cl, due to the effects of the cation exchange.

4.5. Exchangeable Sodium Percentage

[35] Soil samples were collected at 5 depths at the end of each irrigation period and after each winter season to measure the exchangeable cations and the cation exchange capacity (CEC), and to calculate the exchangeable sodium percentage (ESP). ESP was used to evaluate sodification hazards.

[36] In monoliths A and B, the highest ESP values (about 7%) occurred after the irrigation periods (Figure 7). This value does not imply sodification risks since ESP values must be larger than 15% to lead to soil sodicity. However, lower values of ESP (about 10%) in fine-textured soils may lead to clay dispersion and thus affect soil structural stability, reflected by a decrease in hydraulic conductivities and overall deterioration of soil properties. The highest ESP value in the surface layer of monolith C, irrigated with the poorest quality water (C′), was 17% after the last irrigation cycle (September 2003). ESP decreased to about 7% during the following winter (March 2004), still much higher value than the initial condition (Figure 7). Although ESP values decreased in all soil monoliths after the winter rainfall periods, there was a gradual increase in ESP when considered on an annual basis.

[37] Figure 7 shows a comparison between ESPs simulated with HYDRUS-1D and calculated from measured exchangeable sodium concentrations and the CEC at selected times after the irrigation and winter rainfall periods. A good agreement between measured and simulated values was found, particularly for monolith C. Exceptions were ESP values from monolith B which showed relatively large differences for the last three irrigation and rainfall periods (March 2003, September 2003, and March 2004). Still, a

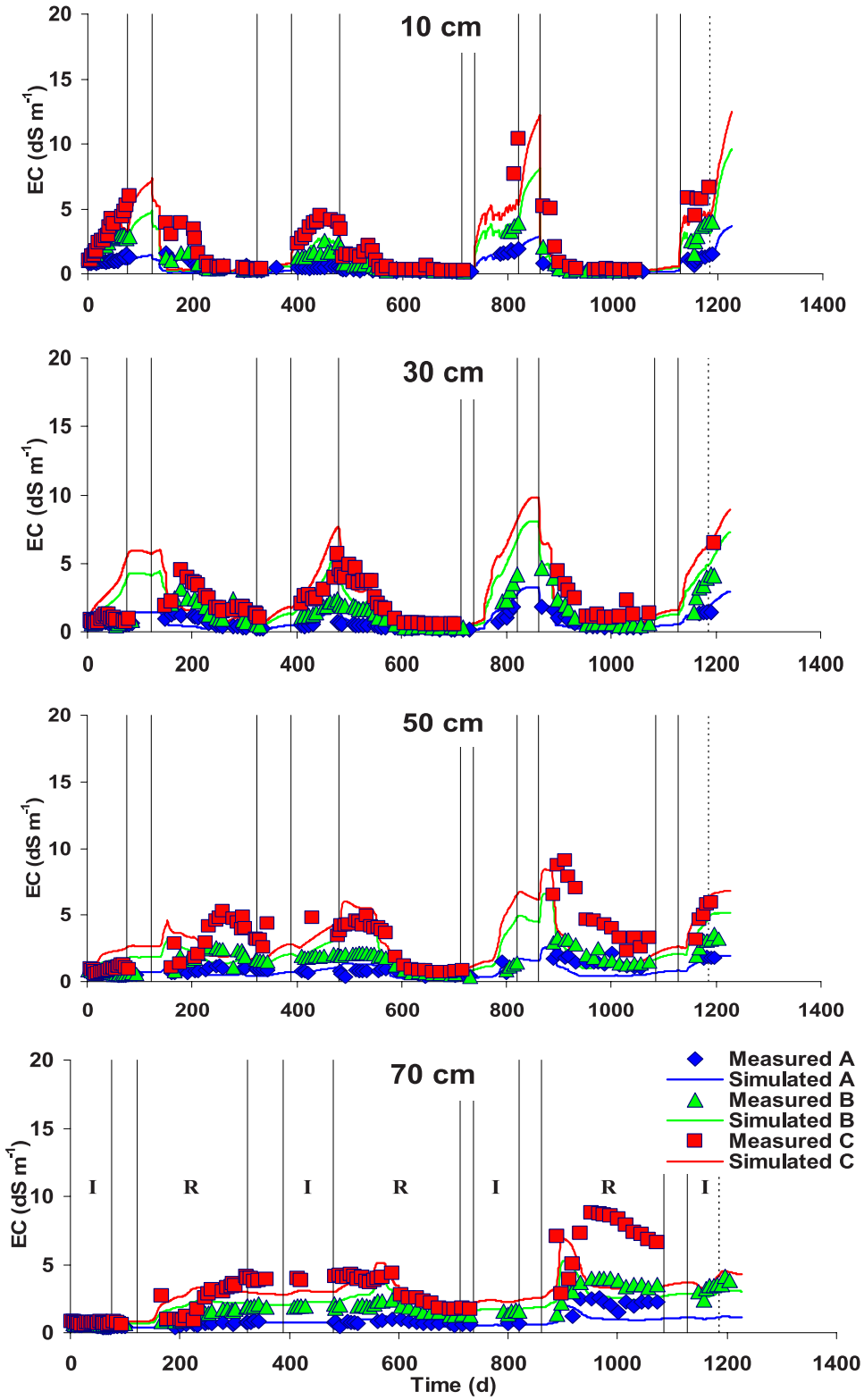

Figure 2. Measured and simulated soil solution electrical conductivities in monoliths A, B, and C. I and R correspond to the irrigation and rainfall periods, respectively.

relatively large R^2 value of 0.76 (n = 120 observations) was obtained for all observations.

4.6. Precipitation-Dissolution of Solid Phases

[38] The highest concentrations of individual cations and anions were recorded in monolith C after the fourth irrigation period and before the start of the rainy season. The HYDRUS model produced during this time period the lowest values of pIAP (negative logarithm of the ion activity product) for both calcite and gypsum. Since the minimum observed pIAP values for calcite and gypsum were 12.6 and 30.3, respectively, while precipitation occurs

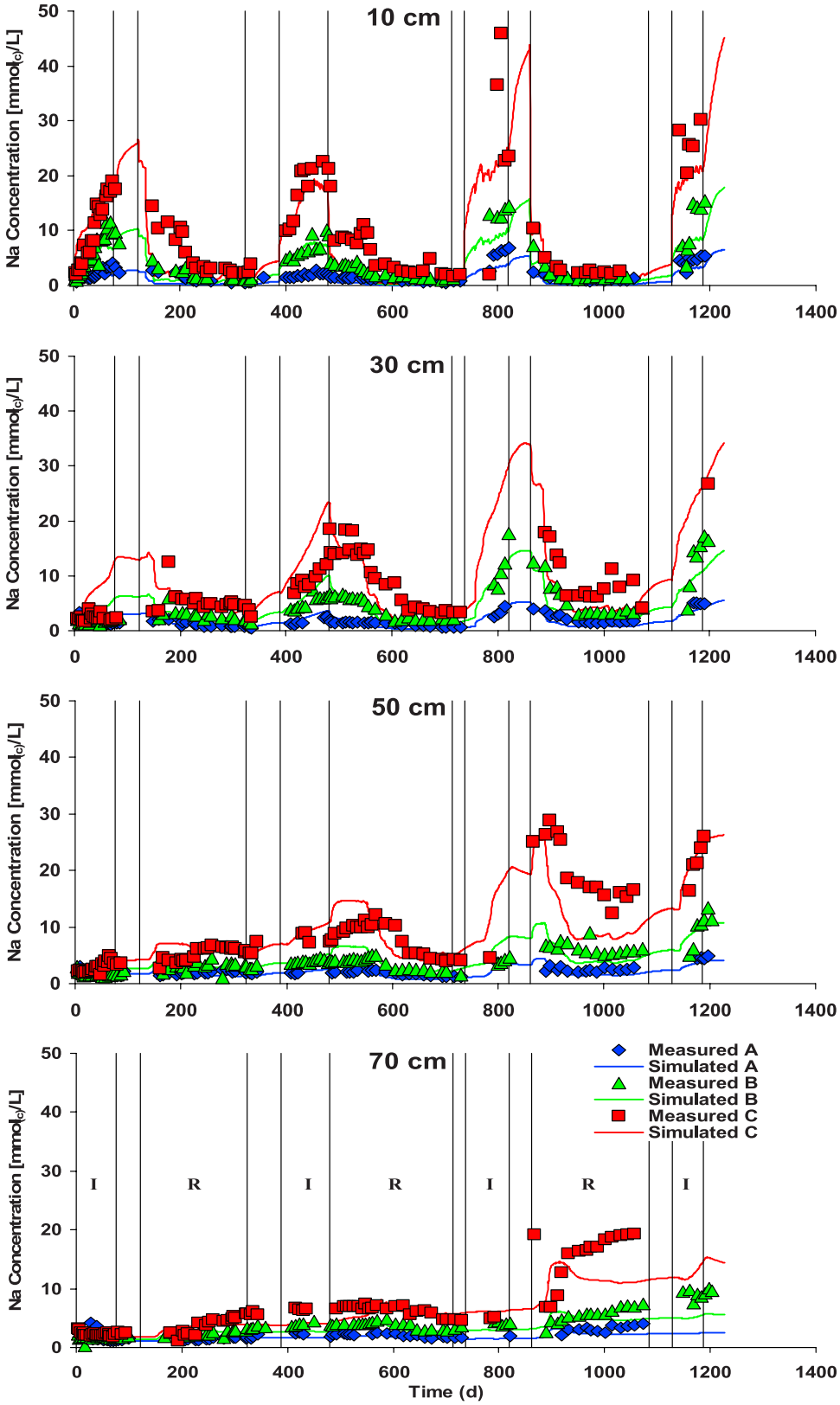

Figure 3. Measured and simulated soluble sodium concentrations in monoliths A, B, and C. I and R correspond to the irrigation and rainfall periods, respectively.

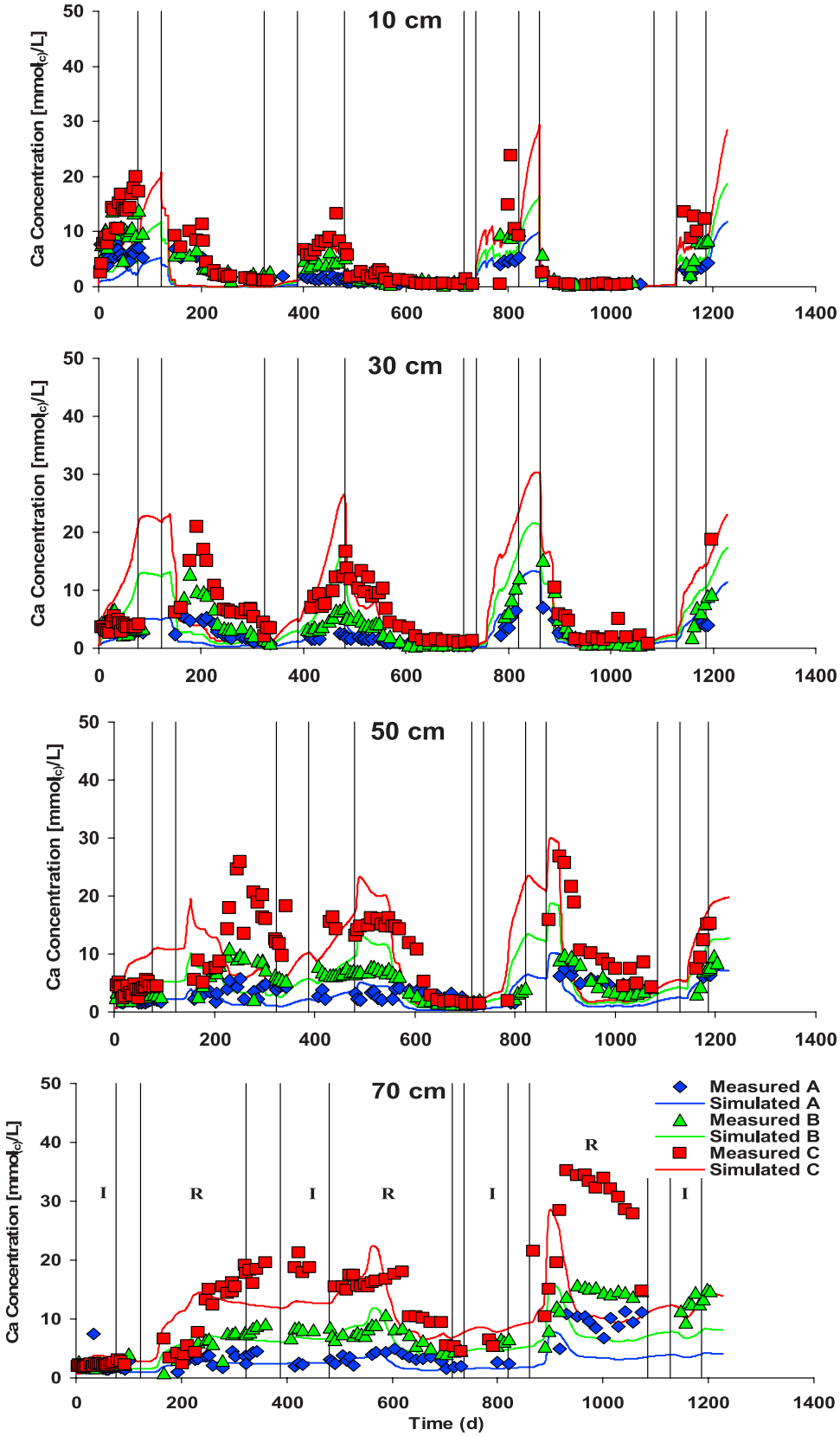

Figure 4. Measured and simulated soluble calcium concentrations in monoliths A, B, and C. I and R correspond to the irrigation and rainfall periods, respectively.

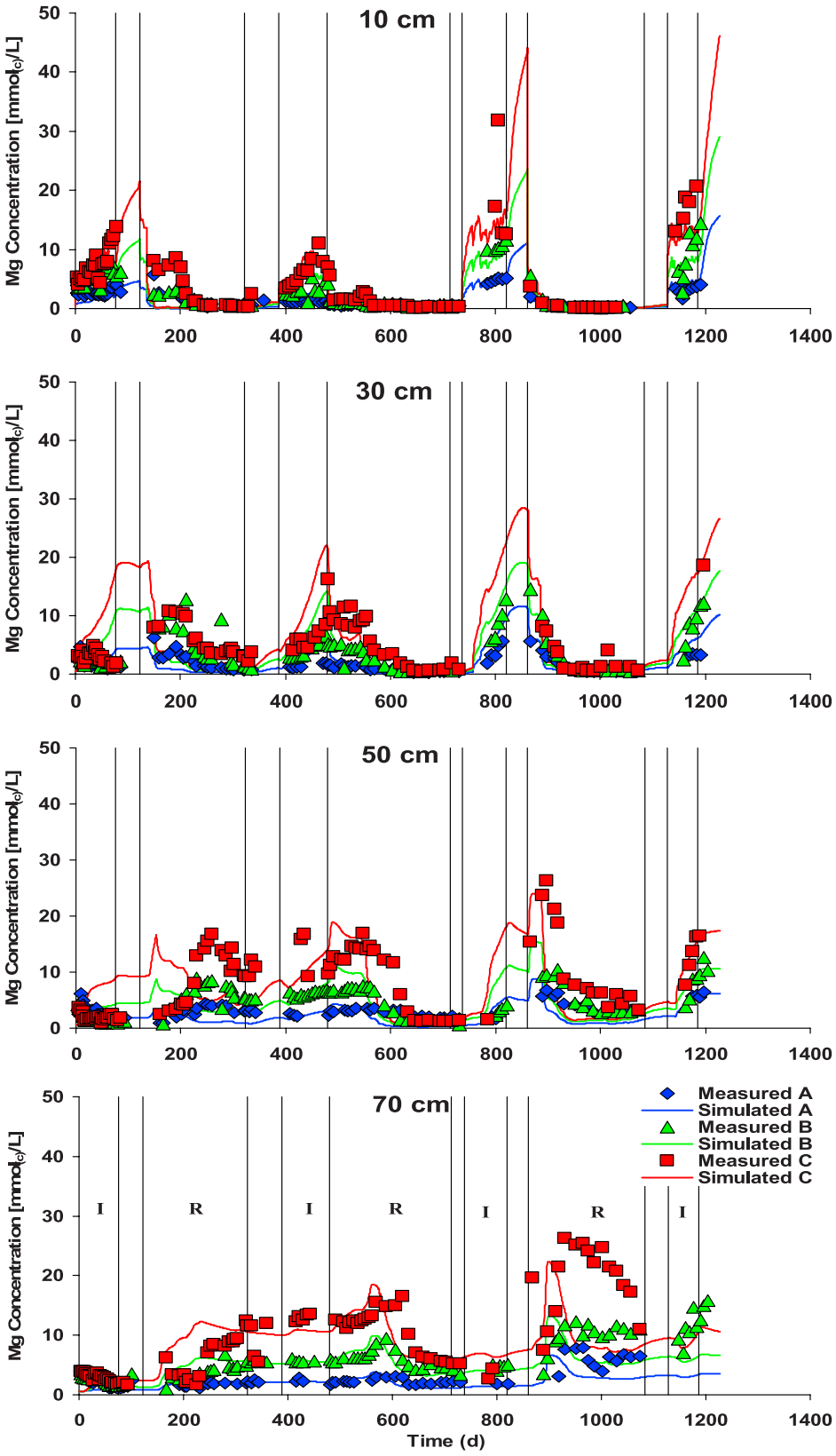

Figure 5. Measured and simulated soluble magnesium concentrations in monoliths A, B, and C. I and R correspond to the irrigation and rainfall periods, respectively.

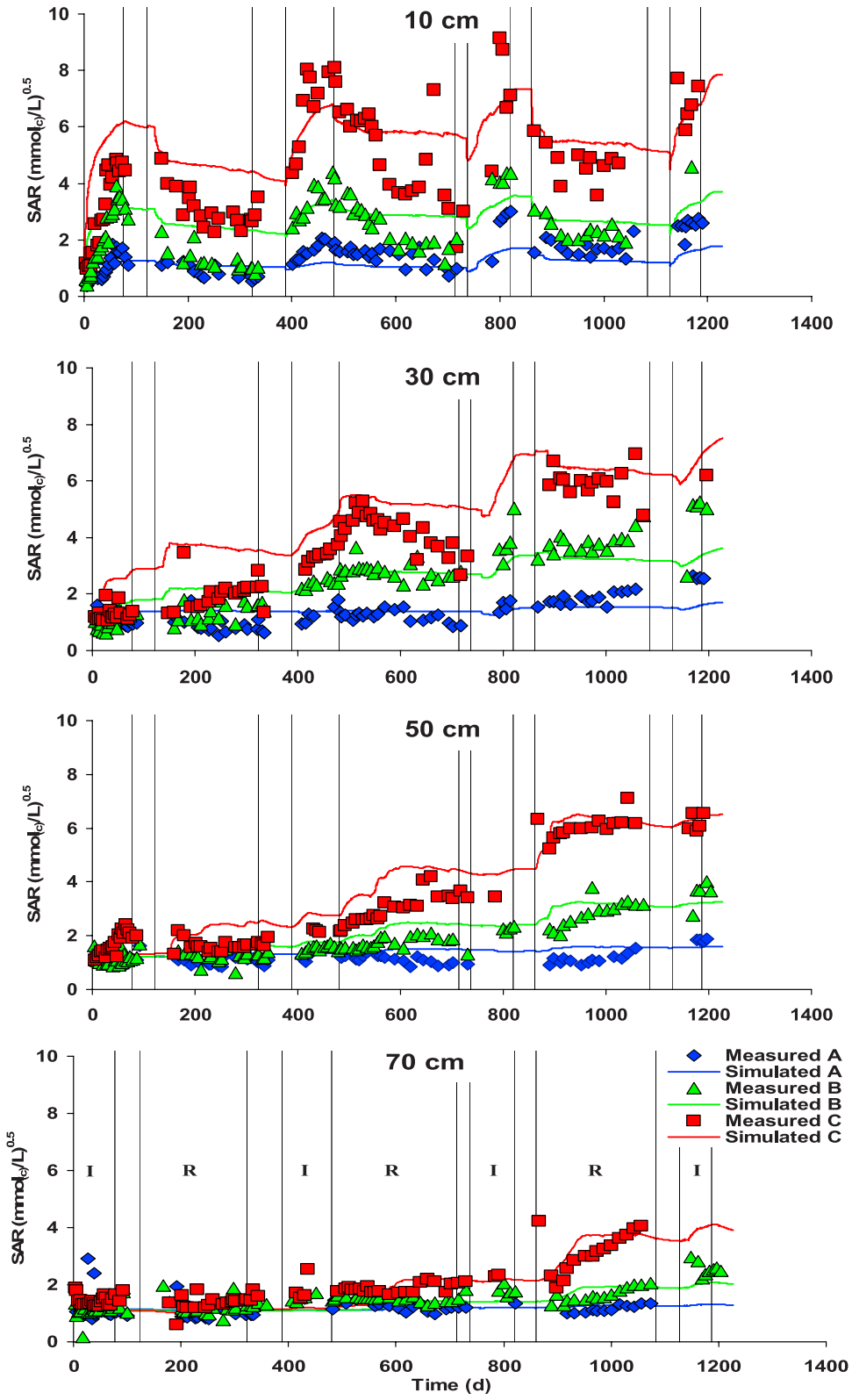

Figure 6. Measured and simulated sodium adsorption ratios (SAR) for monoliths A, B, and C. I and R correspond to the irrigation and rainfall periods, respectively.

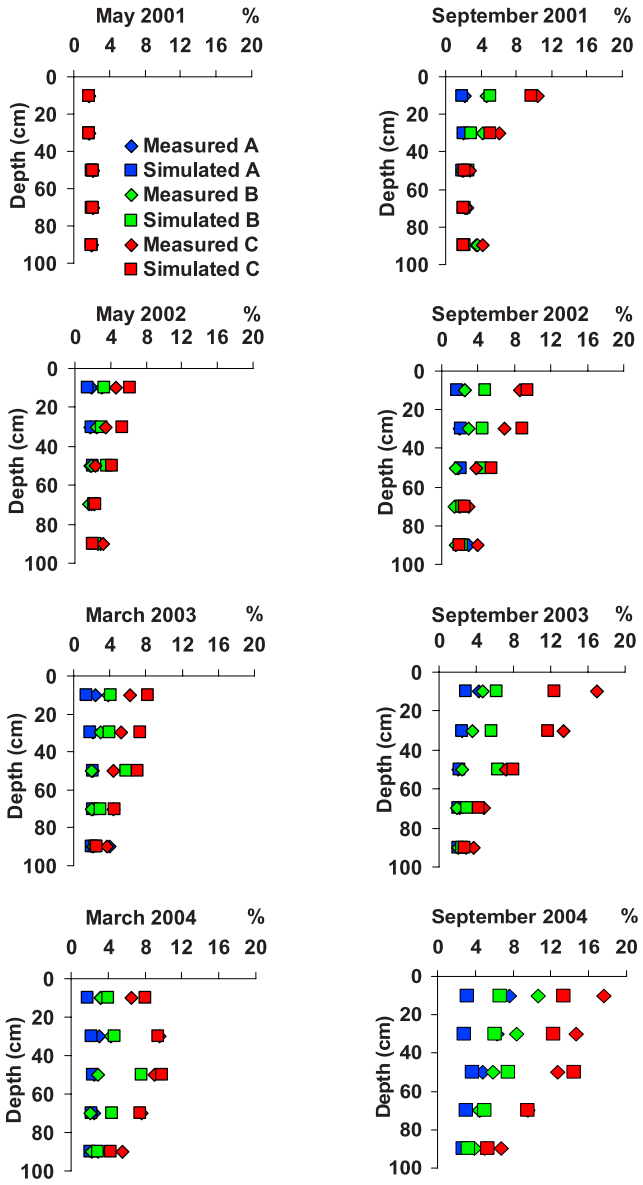

Figure 7. Measured and simulated exchangeable sodium percentages (ESP) for monoliths A, B, and C.

at values of 8.37 and 4.848 [*Truesdell and Jones*, 1974], no precipitation occurred in our lysimeters.

5. Sensitivity Analysis

5.1. Effects of the Osmotic Stress on Root Water Uptake

[39] For the simulations reported above we assumed that the potential root water uptake was reduced due to both water stress (not sufficient supply of water) and salinity stress (high levels of salinity). We further assumed that the effects of the water and salinity (osmotic) stress are additive [*van Genuchten*, 1987]. To describe the root water uptake reductions, we used the model of *Feddes et al.* [1978], which assumes that root water uptake is zero close to saturation (for pressure heads $h > h_1$) and below the wilting point pressure head ($h < h_4$). Water uptake was considered optimal between pressure heads h_2 and h_3, whereas for pressure head between h_3 and h_4 (or h_1 and h_2), water uptake decreases (or increases) linearly with h. In this study, we used parameters suggested by *Wesseling et al.* [1991] for pasture, i.e., $h_1 = -10$ cm, $h_2 = -25$ cm, $h_3 = -200$ to -800 cm, $h_4 = -8000$ cm.

[40] To evaluate the effects of the water and salinity stress on root water uptake we reran the simulation for monolith C without considering osmotic head reductions. Cumulative potential transpiration for the entire 4-year period was equal to 331 cm. This total potential value was reduced due to the pressure head (water) stress to 240 cm and due to combined pressure head and osmotic head stress to 228 cm. The osmotic stress effects on the cumulative root water uptake (transpiration) were thus relatively minor in our lysimeters. The effects of salinity stress on predicted Na concentrations are shown in Figure 8. Since osmotic stress reduces root water uptake, the model predicts larger water contents, and smaller Na concentrations (Figure 8). Predicted Na concentrations are especially lower during the dry periods when lower water contents lead to larger solution concentrations, and thus to larger osmotic heads and more reductions in root water uptake.

5.2. Effects of Solution Composition on the Hydraulic Conductivity

[41] Our simulations thus far assumed that hydraulic conductivities in the soil profile are reduced due to the effects of the solution composition as described by equation (6). To evaluate the effects of these reductions in the hydraulic conductivity on predicted concentrations of the major ions, we reran the simulation for monolith C without considering the hydraulic conductivity reductions. While in our original simulations the hydraulic conductivities were often reduced by up to two orders of magnitude as a result of solution composition changes, the reductions did not lead to dramatically different water content (not shown) or ion concentration (Figure 8) profiles. While large reductions in the hydraulic conductivity certainly will have a dramatic effect on many short-term processes, such as especially ponded infiltration, the effects on long-term (seasonal) processes appear relatively minor when flux-type atmospheric boundary conditions are used (as was the case in our study).

5.3. Effects of Model Complexity

[42] The HYDRUS-1D model as used in this study with the major ion chemistry module is a relatively complex code which requires a large number of input parameters that are not always readily available. This poses the obvious question whether it is necessary to use such a complex model to describe the transport of major ions, or if one could use simpler models and obtain similar results. Our results indicate that neglecting osmotic stress on root water uptake or the effects of salinity on the hydraulic conductivity did lead to very similar results. Since no solid phases precipitated during our experiments, or were added as amendments, we did not need to consider precipitation and dissolution. Could we further simplify the problem by not considering cation exchange and using a much simpler linear K_d (the distribution coefficient between the liquid and solid phase) approach that assumes that particular

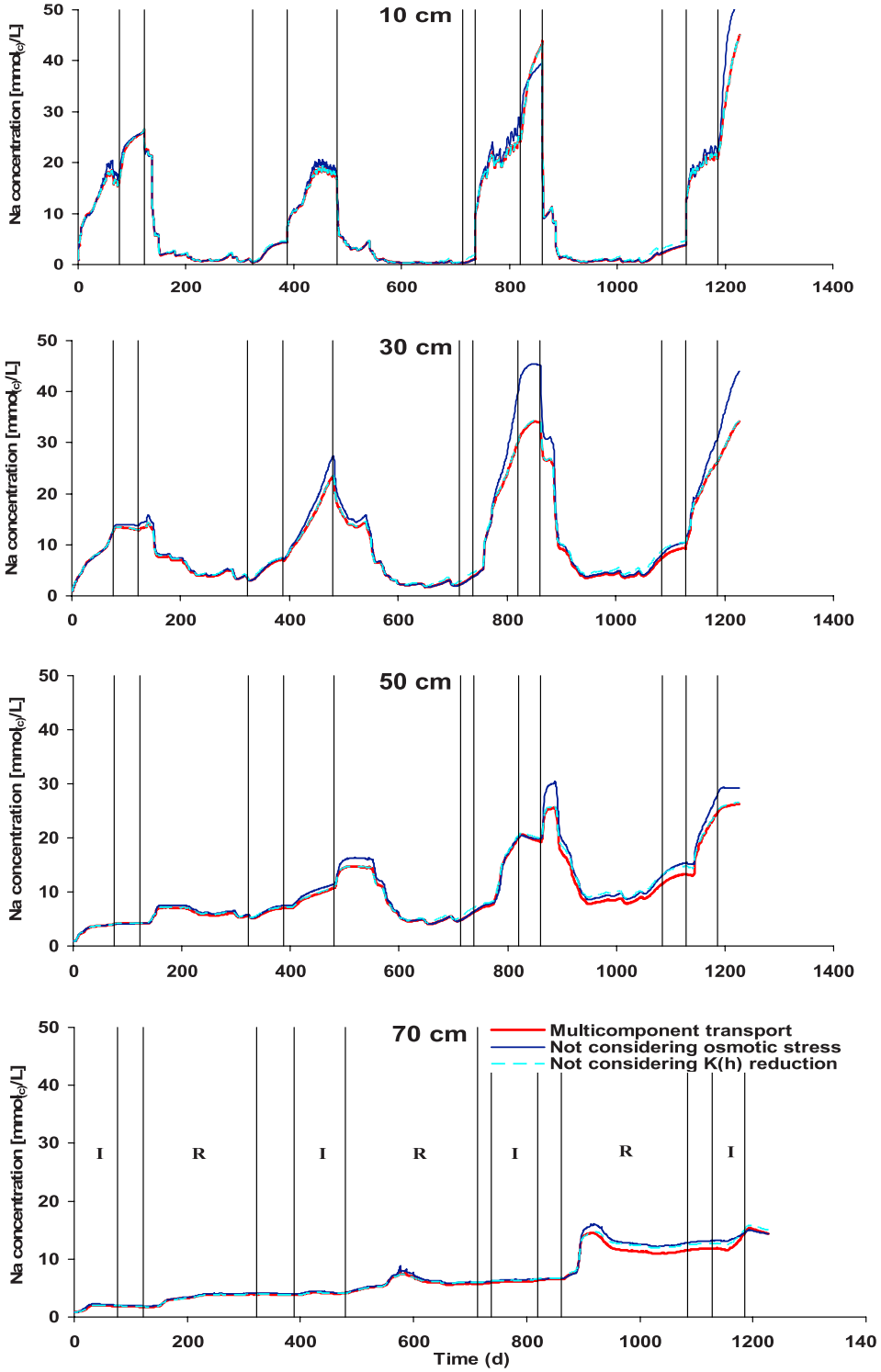

Figure 8. Effects of osmotic stress and reductions in the hydraulic conductivity due to changes in the solution composition on calculated Na^+ concentrations in lysimeter C.

solutes are independent of each other? To answer this question we reran again the simulation for monolith C, but now assumed that cations are transported independently of each other and used distribution coefficients (K_d) equal to either zero (a nonadsorbing tracer) or values obtained by relating the liquid and sorbed concentrations from collected samples. The K_d coefficients obtained in this way for different soil layers varied between 4.8 and 5.55 L kg^{-1} for Na, between 86.5 and 147 L kg^{-1} for Mg, and between 149 and 267 L kg^{-1} for Ca. Sodium concentrations at a depth of 10 cm obtained with three simulations that considered either cation exchange, no sorption (tracer-like

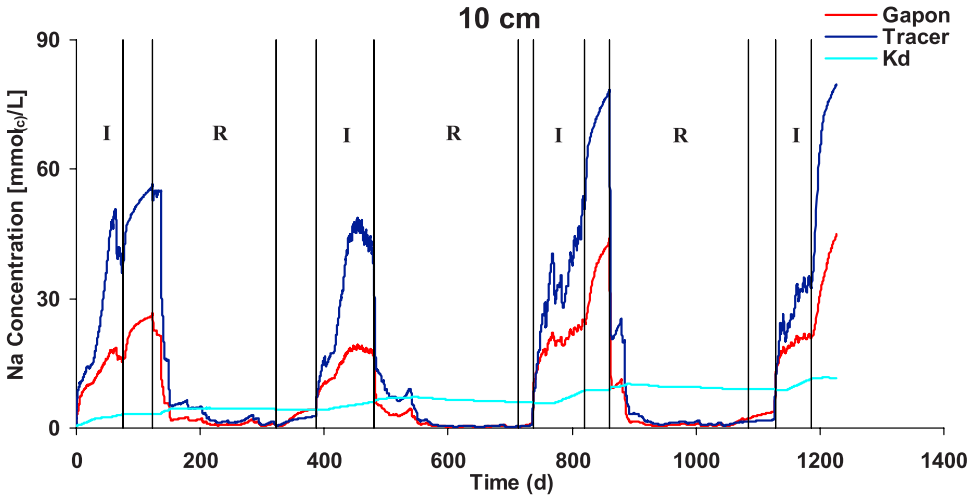

Figure 9. Calculated Na^+ concentrations in lysimeter C using the Gapon exchange equation (equation (2)), using the distribution coefficient K_d approach, and assuming no sorption (tracer).

behavior), or linear sorption are shown in Figure 9. Notice that the three runs produced dramatically different results. Although the solute concentrations obtained with simulations that considered either cation exchange or no sorption showed similar patterns, absolute values of the concentrations were significantly larger for the tracer. Also, the simulations assuming linear sorption completely failed to describe the observed concentration patterns. Hence, while not all options of a complex model always need to be used for a particular data set or application, any simplification of the model by neglecting or simplifying relevant processes must be done with extreme caution.

6. Conclusion

[43] The use of irrigation water with EC values up to 1.6 dS m^{-1} between May 2001 to September 2004 did not lead to salinization/alkalization of the medium-textured Fluvisol because of favorable hydraulic characteristics and winter precipitation. Although the soil salinity at the end of each irrigation cycle gradually increased in the surface layers (0–40/50 cm), reaching a maximum value of about 5 dS m^{-1}, EC values in the upper layers after each rainfall period were reduced down to their initial values. Soil salinity steadily increased below a depth of 40 cm due to leaching of salts from the upper layers, but did not exceed EC values of 3 dS m^{-1}. SAR and ESP values also increased after the application of irrigation water and decreased during the rainfall leaching, but showed a gradual increase from year to year.

[44] Irrigation with water having an EC of 3.2 dS m^{-1} can cause significant soil salinization and alkalization. After two irrigation cycles (in 2003 and 2004), the EC of the soil solution of the surface soil horizon (0–20 cm) increased to about 12 dS m^{-1}, while SAR increased to about 8 $(mmol_{(c)} L^{-1})^{0.5}$, and ESP to 17%. Although the winter rainfall leached most salts from the surface layers, this was not sufficient to restore the soil to its initial conditions bellow a depth of 40 cm. EC values reached 3 dS m^{-1}, SAR 7 $(mmol_{(c)} L^{-1})^{0.5}$ and ESP 9% at a depth of 50 cm in March 2004, immediately after the third rainfall season. The trend of soil salinization/alkalization below 40/50 cm must be taken into account when using continuously poor quality irrigation waters, especially in dry years.

[45] HYDRUS-1D successfully simulated the water regime, as well as the effects of different irrigation waters on the geochemistry of the studied Fluvisol. The correspondence between observed and simulated variables was remarkable, considering that simulations were carried out to predict field measurements over a considerable time period (4 years) without any calibration, and with all input variables (i.e., the soil hydraulic properties, solute transport parameters, atmospheric demand, Gapon constants, physical and chemical characteristics of the soil, LAI and root depth) measured independently. The agreement between measured and simulated values was best for soluble sodium concentrations (R^2 = 0.78), SAR (R^2 = 0.87) and ESP (R^2 = 0.76), while water contents (R^2 = 0.60), ECs (R^2 = 0.65), and soluble magnesium (R^2 = 0.62) and calcium concentrations (R^2 = 0.63) were predicted slightly less well.

[46] Carried out sensitivity analysis showed that model predictions for our experimental conditions were not significantly affected by the reduction of hydraulic conductivities in the soil profile due to the effects of the solution composition or by the reduction of the root water uptake due to osmotic stress. Our results thus indicate that it would be possible for our experimental conditions to simplify the model and to neglect the effect of the osmotic stress on root water uptake or the effect of salinity on the hydraulic conductivity. On the other side, the solute concentrations could not be well predicted without considering cation exchange. Simulations that considered either no or linear sorption completely failed to describe the observed concentration patterns. Although it may not be always necessary to consider all options of a complex model for a particular data set or application, any simplification of the model by neglecting or simplifying relevant processes must be done with extreme caution.

[47] In spite of the considerable input data demands, HYDRUS-1D proved to be an effective tool that may become very useful for irrigation management, and for predicting the effects of irrigation water quality on soil

and groundwater quality. This may be particularly important when designing new irrigation areas. Models such as HYDRUS-1D, after proper calibration and validation, hence should be considered for establishing sound irrigation policies and for mitigating associated environmental risks.

References

Allen, R. G., L. S. Pereira, D. Raes, and M. Smith (1998), Crop evapotranspiration: Guidelines for computing crop water requirements, *Irrig. Drain. Pap.*, *56*.

Arya, L. M., D. A. Farrel, and G. R. Blake (1975), A field study of soil water depletion patterns in presence of growing soybean roots, I. Determination of hydraulic properties of the soil, *Soil Sci. Soc. Am. J.*, *45*, 1023–1030.

Ayers, R., and D. Westcot (1985), Water quality for agriculture, *Irrig. Drain. Pap.*, *29*.

Bouma, J., C. Belmans, L. W. Dekker, and W. J. M. Jeurissen (1983), Assessing the suitability of soils with macropores for subsurface liquid waste disposal, *J. Environ. Qual.*, *12*, 305–311.

Decker, D. L., J. Šimůnek, S. W. Tyler, C. Papelis, and M. Logsdon (2006), Variably saturated reactive transport of arsenic in heap leach facilities, *Vadose Zone J.*, *5*, 430–444.

Dudley, L. M., R. J. Wagenet, and J. J. Jurinak (1981), Description of soil chemistry during transient solute transport, *Water Resour. Res.*, *17*, 1498–1504.

Feddes, R. A., P. J. Kowalik, and H. Zaradny (1978), *Simulation of Field Water Use and Crop Yield*, John Wiley, Hoboken, N. J.

Food and Agricultural Organization (1998), World reference base for soil resources, *World Soil Resour. Rep.*, *84*.

Gonçalves, M. C., F. J. Leij, and M. G. Schaap (2001), Pedotransfer functions for solute transport parameters of Portuguese soils, *Eur. J. Soil Sci.*, *52*, 563–574.

Keren, R. (2000), Salinity, in *Handbook of Soil Science*, edited by M. E. Summer, pp. G1–G26, CRC Press, Boca Raton, Fla.

Mallants, D., M. Vanclooster, M. Meddahi, and J. Feyen (1994), Estimating solute transport in undisturbed soil columns using time domain reflectrometry, *J. Contam. Hydrol.*, *17*, 91–109.

Mass, E. V. (1990), Crop salt tolerance, in *Agricultural Salinity Assessment and Management, Manual Eng. Pract.*, vol. 71, edited by K. K. Tanji, chap.13, pp. 262–304, Am. Soc. of Civ. Eng., Reston, Va.

McNeal, B. L. (1968), Prediction of the effect of mixed-salt solutions on soil hydraulic conductivity, *Soil Sci. Soc. Am. Proc.*, *32*, 190–193.

McNeal, B. L., J. D. Oster, and J. T. Hatcher (1970), Calculation of electrical conductivity from solution composition data as an aid to in-situ estimation of soil salinity, *Soil Sci.*, *110*, 405–414.

Melich, A. (1948), Determination of cations and anions exchange properties of soils, *Soil Sci.*, *66*, 429–445.

Pitzer, K. S. (1973), Thermodynamics of electrolytes I: Theoretical basis and general equations, *J. Phys. Chem.*, *77*, 268–277.

Pitzer, K. S. (1979), Activity coefficients in electrolyte solutions, in *Activity Coefficients in Electrolyte Solutions*, edited by R. M. Pitkowicz, pp.157–208, CRC Press, Boca Raton, Fla.

Richards, L. A. (1954), *Diagnosis and Improvement of Saline and Alkali Soils, Agric. Handb.*, vol. 60, U.S. Dep. of Agric., Washington, D. C.

Robbins, C. W., R. J. Wagenet, and J. J. Jurinak (1980a), A combined salt transport-chemical equilibrium model for calcareous and gypsiferous soils, *Soil Sci. Soc. Am. J.*, *44*, 1191–1194.

Robbins, C. W., R. J. Wagenet, and J. J. Jurinak (1980b), Calculating cation exchange in a salt transport model, *Soil Sci. Soc. Am. J.*, *44*, 1195–1200.

Russo, D. (1986), Simulation of leaching of a gypsiferous-sodic desert soil, *Water Resour. Res.*, *22*, 1341–1349.

Russo, D. (1988), Numerical analysis of the nonsteady transport of interacting solutes through unsaturated soil: I. Homogeneous systems, *Water Resour. Res.*, *24*, 271–284.

Russo, D., and E. Bresler (1977), Analysis of the saturated–unsaturated a hydraulic conductivity in a mixed Na–Ca soil system, *Soil Sci. Soc. Am. J.*, *41*, 706–710.

Shainberg, I., and G. J. Levy (1992), Physico-chemical effects of salts upon infiltration and water movement in soils, in *Interacting Processes in Soil Science*, edited by R. J. Wagenet, P. Baveye, and B. A. Stewart, CRC Press, Boca Raton, Fla.

Šimůnek, J., and D. L. Suarez (1994), Two-dimensional transport model for variably saturated porous media with major ion chemistry, *Water Resour. Res.*, *30*, 1115–1133.

Šimůnek, J., and D. L. Suarez (1997), Sodic soil reclamation using multicomponent transport modeling, *J. Irrig. Drain. Eng.*, *123*(5), 367–376.

Šimůnek, J., and A. J. Valocchi (2002), Geochemical transport, in *Methods of Soil Analysis,* part 1, *Physical Methods*, 3rd ed., edited by J. H. Dane and G. C. Topp, chap. 6.9, pp. 1511–1536, Soil Sci. Soc. of Am., Madison, Wis.

Šimůnek, J., D. L. Suarez, and M. Šejna (1996), The UNSATCHEM software package for simulating one-dimensional variably saturated water flow, heat transport, carbon dioxide production and transport, and multicomponent solute transport with major ion equilibrium and kinetic chemistry, version 2.0, *Res. Rep. 141*, 186 pp., U. S. Salinity Lab., Agric. Res. Serv., Riverside, Calif.

Šimůnek, J., M. T. van Genuchten, and M. Šejna (2005), The HYDRUS-1D software package for simulating the one-dimensional movement of water, heat, and multiple solutes in variably-saturated media, version 3.0, *HYDRUS Software Ser. 1*, 270 pp., Dep. of Environ. Sci., Univ. of Calif., Riverside.

Steppuhn, H., M. T. van Genuchten, and C. M. Grieve (2005), Root-zone salinity: II. Indices for tolerance in agricultural crops, *Crop Sci.*, *45*, 221–232.

Suarez, D. L., and J. Šimůnek (1997), UNSATCHEM: Unsaturated water and solute transport model with equilibrium and kinetic chemistry, *Soil Sci. Soc. Am. J.*, *61*, 1633–1646.

Toride, N., F. J. Leij, and M. T. van Genuchten (1995), The CXTFIT code for estimating transport parameters from laboratory or field tracer experiments, version 2.0, *Res. Rep. 137*, U.S. Salinity Lab., Riverside, Calif.

Truesdell, A. H., and B. F. Jones (1974), Wateq, a computer program for calculating chemical equilibria of natural waters, *J. Res. U.S. Geol. Surv.*, *2*(2), 233–248.

van Genuchten, M. T. (1980), A closed form equation for predicting the hydraulic conductivity of unsaturated soils, *Soil Sci. Soc. Am. J.*, *44*, 892–898.

van Genuchten, M. T. (1987), A numerical model for water and solute movement in and below the root zone, *Res. Rep. 121*, U.S. Salinity Lab., Agric. Res. Serv., Riverside, Calif.

van Genuchten, M. T., and J. Šimůnek (2004), Integrated modeling of vadose zone flow and transport processes, in *Unsaturated Zone Modelling: Progress, Challenges and Applications, Frontis Ser.*, vol. 6, edited by R. A. Feddes, G. H. de Rooij, and J. C. van Dam, pp. 37–69, Springer, New York.

van Genuchten, M. T., F. J. Leij, and S. R. Yates (1991), The RETC code for quantifying the hydraulic functions of unsaturated soils, *Rep. EPA/600/2-91-065*, U.S. Environ. Prot. Agency, Washington, D. C.

Van Lierop, W. (1990), Soil pH and lime requirement determination, in *Methods of Soil Analysis*, part 2, 2nd ed., edited by A. L. Page, R. H. Miller, and D. R. Keeney, pp. 76–120, Soil Sci. Soc. of Am., Madison, Wis.

Wagenet, R. J., and J. L. Hutson (1987), LEACHM: Leaching Estimation and Chemistry Model, a process-based model of water and solute movement, transformations, plant uptake and chemical reactions in the unsaturated zone, continuum 2, report, Water Resour. Inst., Cornell Univ., Ithaca, N. Y.

Wesseling, J. G., J. A. Elbers, P. Kabat, and B. J. van den Broek (1991), SWATRE: Instructions for input, report, Winand Staring Cent., Wageningen, Netherlands.

White, N. L., and L. M. Zelazny (1986), Charge properties in soil colloids, in *Soil Physical Chemistry*, edited by D. L. Sparks, pp. 39–81, CRC Press, Boca Raton, Fla.

M. C. Gonçalves, J. C. Martins, M. J. Neves, F. P. Pires, and T. B. Ramos, Department of Soil Science, Estação Agronómica Nacional, Avenida República, P-2784-505 Oeiras, Portugal. (mc.goncalves@netc.pt)

J. Šimůnek, Department of Environmental Sciences, University of California, Riverside, CA 92521, USA.